Development and Evaluation of Sensor-Powered Wireless Smart Wooden Panels

Yuning Su
Simon Fraser University
Burnaby, BC, Canada
yuning_su@sfu.ca

Bofan Yu
Simon Fraser University
School of Computing Science
Burnaby, British Columbia, Canada
bofany@sfu.ca

Tingyu Zhang
Simon Fraser University
Burnaby, BC, Canada
tza80@sfu.ca

Yonghao Shi
Simon Fraser University
Burnaby, BC, Canada
yonghao_shi@sfu.ca

Te-Yen Wu
Florida State University
Tallahassee, FL, United States
tw23l@fsu.edu

Xing-Dong Yang
Simon Fraser University
Burnaby, BC, Canada
xingdong_yang@sfu.ca

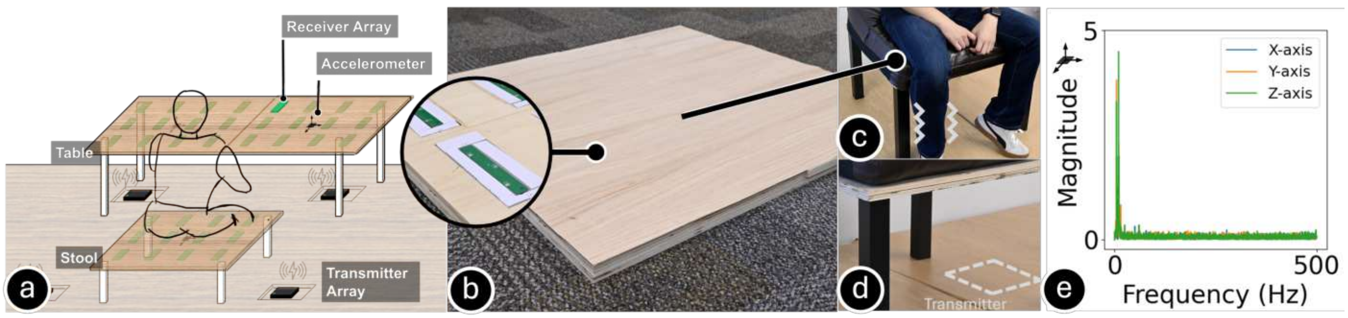

Figure 1: AccelLumber demonstrates the technical feasibility of wireless smart wooden panels using commodity sensors, electronics, and wireless power transfer systems. (a) Conceptual illustration of furniture built with AccelLumber panels, wirelessly powered by RF transmitters embedded beneath the floor. (b) An AccelLumber panel equipped with embedded receiver antennas that supply power to integrated components, including a microcontroller (MCU), Bluetooth Low Energy (BLE) module, and sensors such as a 3-axis accelerometer. (c) A cushioned stool built with AccelLumber captures stress-related behaviors such as leg shaking while seated. (d) The stool panel wirelessly harvests RF energy from the floor-embedded transmitter. (e) Corresponding raw accelerometer data showing the detected leg-shaking activity.

Abstract

We explored the technical feasibility of wireless smart wooden panels that integrate conventional sensors and electronics. Prior work has explored either embedding wired, off-the-shelf electronic components in wood or enabling wireless energy transfer, but supporting both simultaneously using existing technology has remained uncertain. Addressing this gap is important for moving smart wooden panels from conceptual visions to practical applications. Following a validation-through-implementation approach, we developed a prototype that leverages a commodity RF-based wireless power transfer (WPT) system to continuously power off-the-shelf sensors (e.g., accelerometers) and electronic components (e.g., MCUs, BLE modules) within wooden furniture panels. We evaluate its performance across three dimensions: panel scalability (how different-sized panels reliably operate embedded sensors), power infrastructure requirements (the number and placement of RF transmitters needed for continuous operation), and activity recognition. Our results demonstrate that wireless smart wooden panels are not merely a conceptual idea, but a viable approach to realizing smart environments.

CCS Concepts

• **Human-centered computing** → *Interaction devices.*

Keywords

Smart Environment, RF

ACM Reference Format:
Yuning Su, Bofan Yu, Tingyu Zhang, Yonghao Shi, Te-Yen Wu, and Xing-Dong Yang. 2018. Development and Evaluation of Sensor-Powered Wireless Smart Wooden Panels. In *Proceedings of Graphics Interface 2026 (GI '26).* ACM, New York, NY, USA, 14 pages. https://doi.org/XXXXXXX.XXXXXXX

GI '26, June 9–12, 2026, Waterloo, Ontario, Canada

ACM ISBN 978-1-4503-XXXX-X/18/06
https://doi.org/XXXXXXX.XXXXXXX

1 INTRODUCTION

Recent advances in ubiquitous computing have sparked growing interest in smart wooden panels [24, 26, 40, 43, 56, 68]. By embedding sensors into wood surfaces, these panels can capture everyday activities, such as eating, working, through signals like vibration [56, 68] and motion [63]. When integrated into furniture, they preserve the familiar aesthetic and tactile qualities of wood while extending furniture functionality through digital sensing. This approach offers a promising path for 'weaving' sensing into everyday objects. Yet, a key question remains: is it technically feasible to build sensor-powered wooden panels with current technologies? Addressing this question is critical for moving beyond conceptual visions and toward practical applications.

Prior work has embedded sensors and core electronics, such as microcontrollers (MCUs) and Bluetooth Low Energy (BLE) modules, directly into wooden panels [24, 26, 43, 56, 68]. However, these systems typically rely on wired power, making panels tethered, cumbersome, and difficult to scale. More recent efforts explored wireless operation via ultra–low-power platforms such as RFID [58]. While this removes wiring, it limits functionality. Standard electronics and conventional sensors, which demand higher power, cannot be supported. Consequently, sensing modalities previously demonstrated as useful in smart home applications, like motion [56, 68, 74], are missing in these wireless systems. Beyond the integration of conventional components and power delivery, practical considerations also remain open, particularly in furniture contexts, such as determining the necessary power infrastructure (e.g., the number and placement of wireless power transmitters) to ensure continuous operation across a room space, and assessing how wireless wooden panels can be scaled to different shapes and sizes to accommodate diverse furniture forms.

In this work, we validate the technical feasibility of the *wireless* wooden panel through a proof-of-concept implementation, a common method for validating new concepts [22]. We demonstrate how commodity RF-based wireless power transfer (WPT) devices, though not originally designed for smart wooden panels, can be leveraged to continuously power conventional motion sensors (e.g., accelerometers) and components (e.g., MCUs, BLE) embedded within them. Using standard, off-the-shelf sensors and components offers several benefits. It increases flexibility for incorporating established sensing techniques, supports on-board computation, and enables secure wireless communication via standard platforms. These capabilities could potentially simplify the development of real-world applications for smart wooden panels.

Our prototype (called AccelLumber) was built on a commercial WPT platform (Powercast [50]) and an accelerometer (ADXL335) paired with a system-on-chip (nRF52840) integrating an MCU, ADC, and BLE module. Receiver antennas were embedded in wooden panels to harvest energy from RF transmitters at room-scale distances. Through experiments examining the effect of receiver antenna spacing on energy harvesting efficiency, we refined the system to achieve improved performance. We used this prototype to characterize the performance of the AccelLumber panel when integrated into common furniture with open-bottom flat surfaces, such as tables and stools. Our studies addressed three key feasibility dimensions: (1) Panel scalability - whether rectangular panels of varying sizes can reliably power embedded sensors and components across diverse furniture designs (Section 4), (2) Power infrastructure requirements - the number and configuration of RF transmitters needed to ensure the continuous operation of AccelLumber-powered furniture across a room (Section 4), and (3) Activity recognition — whether AccelLumber-powered furniture can accurately detect common user activities motion sensing (Section 6).

In our study, we also considered practical power-infrastructure scenarios, where power devices and wiring are often installed beneath floors or ceilings for safety and aesthetic reasons. We positioned the RF transmitter beneath the floor (Figure 1a), a strategic decision, as floor placement could be as effective as ceiling placement for RF transmitters but has been largely unexplored. Horizontal furniture surfaces that are well-suited for integrating receiver antennas, such as tabletops or stool seats, are often obstructed from above (e.g., by objects on a table or by seated users), and in these scenarios, under-floor transmitters can provide reliable coverage.

Our study results show that for typical furniture heights (e.g., 50 cm for chairs, 80 cm for tables), only four receiver antennas are sufficient to continuously power electronics (5.98 mW in our implementation). AccelLumber panels with these arrays can be as compact as $36cm \times 46cm$ and scale to different sizes and shapes with additional receivers, allowing flexible adaptation to varying furniture dimensions. Moreover, AccelLumber panels can be powered with transmitters positioned outside the panel's footprint. For example, a tabletop panel with a 3×4 receiver array (72 cm wide in our implementation) can be reliably powered anywhere in a room using under-floor transmitters spaced roughly 1.2 m apart. This suggests that in a typical $6m \times 6m$ room, a 5×5 transmitter array ensures continuous coverage. Finally, evaluations using a smart desk and stool built with AccelLumber panels across 13 daily activities, including appliance use, power tool operation, cooking, and stress behaviors, such as leg shaking (Figure 1d), achieved 95% recognition accuracy.

The main contribution of this work is the validation of the technical feasibility of wireless smart wooden panels that integrate commodity sensors, electronics, and wireless power harvesting. Our results demonstrate that wireless smart wooden panels are not just a conceptual vision, as often assumed, but a technically viable and promising approach for building future interactive furniture and smart environments.

2 RELATED WORK

This section reviews the existing research on the development of smart environments, wood panels with integrated sensing capabilities, and indoor energy harvesting techniques.

2.1 Development of Smart Environments

Smart environments are physical spaces embedded with computational elements and user interfaces designed to enhance quality of life, optimize resource use, and deliver personalized services [11, 44]. In the context of user interfaces, sensors are crucial as they gather user input and activity data, which are essential for enabling ubiquitous computing applications. Unlike approaches that instrument the user's body, such as wearing a smartwatch, instrumenting the physical environment complements wearable devices by addressing some of their key limitations. For example, wearable sensors may struggle to detect activities that do not primarily involve the movement of a specific body part (e.g., the hand) or that may not involve any body movement at all, such as operating household appliances like a microwave. Instrumenting the physical environment and furniture can also complement wearables by sensing contextual information inherent to furniture, such as distinguishing which piece of furniture the user has interacted with. From a user experience perspective, instrumenting furniture has the potential to free users from the need to wear devices in order to capture their interactions with the environment.

The traditional approach to creating smart environments involves instrumenting existing non-smart physical spaces with sensors [16, 19, 23, 32, 74, 75]. Most existing work in this area follows this method. Examples include installing electromagnetic (EM) sensors [10, 16, 32, 55, 76], vibration sensors [23, 75], and light sensors [30, 34, 71] to detect and monitor user interactions and activities. Specifically, StarLight [34] uses photodiodes installed on the ground to receive light signals and reconstruct human posture. Wall++ [76] utilizes antennas and sensors embedded in walls to capture airborne electromagnetic interference (EMI) signals, allowing for the detection and localization of house appliances. Vibration sensors have been installed on ground and walls [75], as well as on plumbing, gas, and HVAC infrastructure [74] to monitor user activities. Additionally, ElectriSense [16] instruments power outlets with sensors to detect appliance usage based on electromagnetic interference in power lines.

In the context of smart wood furniture, the common approach is still to augment existing wooden objects or furniture with sensors [14, 18, 25, 27, 28, 47, 59, 70]. For instance, research has investigated detecting people falling by placing vibration sensors on wooden floors [54]. Additionally, previous research has investigated the creation of smart wooden tables or countertops by attaching vibration sensors to these things to detect users' touch or gesture input [19, 46, 68, 69]. Similarly, commodity smart speakers, such as the Amazon Echo, could potentially achieve comparable sensing capabilities when placed within a physical environment. However, like the approaches discussed above, these methods involve adding external devices to the environment, which may not fully blend into their surroundings.

2.2 Wood Panels with Integrated Sensing Capabilities

Our research is situated within the broader field of computational materials [2], which involves embedding computational capabilities or sensors into everyday materials such as wood, paper, and textiles [3, 6, 14, 45, 47, 49, 66, 67, 71]. Specifically, our work is most relevant to the development of wood panels with integrated sensing capabilities designed for creating interactive furniture and home infrastructures [56, 58, 68].

Prior research primarily focuses on embedding sensors to create interactive wooden surfaces that detect user input and inform daily activities. For instance, iWood integrates vibration sensing into plywood to identify activities like writing or food preparation [68]. The initial prototype was vulnerable to electromagnetic noise due to inadequate shielding. Later work addressed this limitation, enhancing its suitability for real-world applications [56].

A significant limitation of this line of work is that they often require wired connections and external power sources, such as batteries, for sensor operation and data communication. This reliance complicates the traditional woodworking process and demands electrical wiring skills that woodworkers may lack. Additionally, the need for battery charging creates further inconvenience. To address these challenges, Su et al. [58] developed a smart wood panel that functions wirelessly and without a battery, using a grid of RFID tags. However, the limited power that can be harvested from RFID constrains the sampling rate (capped at 2 Hz) and sensing capabilities. The energy harvested is insufficient to power even a basic sensor circuit with a microcontroller and wireless communication units. As a result, their plywood sensor can only detect the presence of objects by monitoring changes in RF signal strength due to occlusion of the RFID tags, with a sampling rate of 2 Hz or lower.

Despite prior efforts, there is still no concrete evidence that smart wooden panels have advanced beyond a conceptual idea. Our research addresses this gap by presenting a functional prototype and a series of experiments, demonstrating that wireless smart wooden panels with commodity sensors and electronic devices are technically feasible.

2.3 Indoor Energy Harvesting

Existing research on indoor energy harvesting explores diverse methods. Our review focuses on solar and RF energy sources. Other approaches frequently discussed in the literature, such as mechanical motion [38], nano-vibrations using triboelectric nanogenerators (TENG) [65], acoustic energy [48], thermoelectric generation [60], and water or gas flow [20], are excluded from this discussion. These methods typically yield only microwatt-scale power, insufficient for high-rate data transmission (e.g., TENG-based [9] and acoustic [51]), or depend on intermittent environmental events (e.g., motion [61] or water/gas flow [37]). As a result, they cannot reliably support continuous sensing and real-time feedback in smart wood panels.

3 SYSTEM DESIGN AND IMPLEMENTATION

photovoltaic (PV) harvesting leverages light to power interactive systems [36]. One research direction explores wireless laser power delivery. For example, Su et al. [57] used lasers to wirelessly power vibrotactile devices for AR/VR, where PV cells convert laser energy into electricity. This approach eliminates batteries and electronics, enabling compact haptic interfaces. In contrast, ambient-light PV systems aim to harness naturally available light to create self-sustaining environments. Pearce et al. [42] introduced PV-Tiles, which combine PV harvesting with digital interface elements to form aesthetically integrated, self-powered surfaces. Xu et al. [72] developed OptoSense, a self-sustained system that uses ambient light both for power and activity sensing. However, a key limitation of PV systems, especially in our context, is occlusion. When PV cells are embedded under wood, energy output drops substantially. In our tests, covering an SP3-37 PV cell with wood grain paper (to

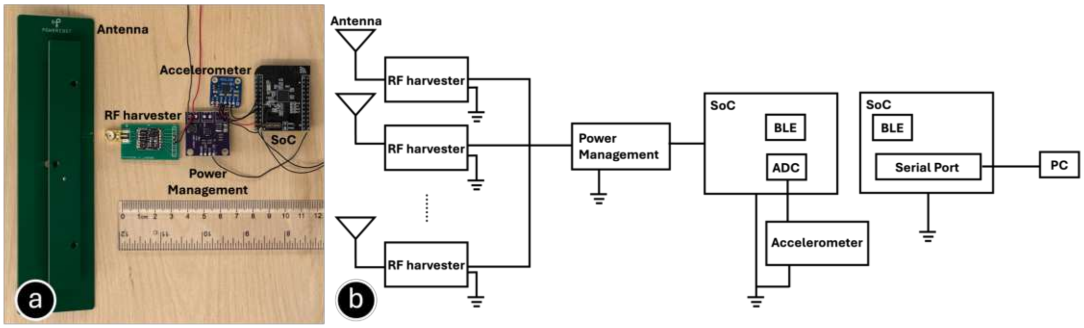

Figure 2: (a) Labeled top view of AccelLumber's electronic components, including the antenna, Powercast RF harvester (P2110), power management unit (BQ25570), accelerometer (ADXL335), and SoC (nRF52840). For clarity, only one antenna and RF harvester pair is shown (detached for better visibility). (b) Circuit diagram illustrating the major component blocks.

preserve a wood-like aesthetic) reduced its output to 0.6% of the uncovered performance at 370 lux illumination.

RF-based approaches have also been widely adopted in self-powered systems, particularly in IoT. Hsieh et al. [21] introduced RFTouchPads, batteryless modular touch sensors powered by ultra-high frequency RFID, which enable touch sensing without external power. Similarly, Gupta et al. [15] developed ForceSticker, an ultra-thin, flexible force sensor powered by RF energy. Their hybrid analog-digital backscatter method allows wireless, batteryless force data transmission via RFID. Despite their promise, backscatter-based harvesting presents several limitations for interactive systems requiring commodity wireless data communication and onboard computation. Communication typically depends on specialized readers [1, 52, 73], which are uncommon in laptops and other consumer devices. Security is also limited in many backscatter systems [7, 52, 62], restricting deployment in real-world applications. Furthermore, continuous onboard computation and bidirectional communication, critical for real-time feedback, are difficult to achieve with backscatter, leaving output capabilities largely unsupported.

Recent advances in wireless power transfer (WPT) have increased the amount of power that can be wirelessly harvested, with several commercial systems now available (e.g., Powercast [50]). Resonant inductive coupling [4], common in smartphones, and electromagnetic induction [33] are effective at short ranges but quickly lose efficiency with distance. These FCC-approved methods are widely adopted for close-range applications but less suitable for furniture surfaces, such as tabletops positioned up to 80 cm above the floor. In contrast, magneto-quasistatic coupling can deliver over 50 W across distances up to 1.5 m [53], offering strong potential for fully wireless sensing and interactive systems in indoor environments.

We demonstrate the feasibility of wireless smart wood panels by implementing AccelLumber on a commodity wireless power transfer system (Powercast [50]). This platform was originally designed for low-power applications without real-time sensing, output, or data communication. While the harvested power is lower than systems such as [53], it is sufficient to operate the device at 5.98 mW. Importantly, AccelLumber leverages an FCC-approved platform, providing a practical pathway for wireless smart wood applications.

Our system integrates an energy-harvesting unit within the wooden panel. This unit consists of an array of RF receiver antennas that capture RF energy from underfloor transmitters, providing power to a low-power, 3-axis accelerometer (ADXL335) and a system-on-chip (SoC, nRF52840) integrating BLE, an MCU, and multiple 12-bit ADCs. Figure 2 shows the PCBs and schematic of our prototype. To support the high sampling rate of the accelerometer, the ADC operates at 1 kHz, capturing vibration signals up to 1 kHz per axis. For consistency and scalability, 12-bit ADC data is padded to 16 bits, resulting in a total sensing throughput of $16bits \times 1kHz \times 3$ channels, yielding a data throughput of 48 kbps. Total power consumption is approximately 5.98 mW (1.81 mA at 3.3 V), with 5.02 mW for the SoC and 0.96 mW for the accelerometer, measured using the Power Profiler Kit II (Nordic). Specifically, the SoC draws 5.02 mW with BLE active (TX power 0 dBm) and 3.56 mW without BLE. This 5.98 mW power budget supports continuous operation of the entire system. Alternatively, the system can be configured for periodic operation, pausing to charge whenever the input power drops below this threshold. In our experiments, we used the full 5.98 mW to characterize the system's performance under its maximum power requirements.

3.1 Antenna Array

The antenna array consists of Powercast 915 MHz receiver antennas. Each antenna is individually rectified using RF harvesters (Powercast P2110) and then DC-combined, which increases tolerance to phase and angle variations. The resulting DC output charges a 1 F supercapacitor via a power management unit (TI BQ25570), providing energy to the SoC and accelerometer. The antennas are arranged in a uniform grid layout, where spacing between neighboring antennas is a key design consideration, as it directly affects the array's overall energy-harvesting efficiency. While larger spacing may reduce interference, it also increases the array's footprint, potentially resulting in unnecessarily large panel sizes and limiting the adaptability of AccelLumber panels for furniture components of various sizes. We conducted two experiments to evaluate the effect of receiver-antenna spacing on energy-harvesting efficiency (see Appendix B for details). Based on the results, we adopted 23 cm longitudinal (long-axis) and 18 cm lateral (short-axis) center-to-center spacing for our implementation. The receiver antennas are organized in a star topology with the SoC at the center, enabling the panel to be cut into different sizes and shapes with minimal impact on performance, as long as the central electronics remain intact.

3.2 Wood Panel

For the final AccelLumber panel, we integrated antennas into a two-layer plywood panel structure (Figure 3). The bottom layer, 1.27 cm thick, functions as the supporting base, with antennas securely attached using both glue and mortise-and-tenon joints. Grooves were also created to accommodate the antennas. The top layer, made from a similar plywood panel, contains rectangular cutouts that hold the patch antennas. These cutouts provide additional support, ensuring the antennas remain securely positioned within the plywood structure. We then used polystyrene boards to fill the gaps between the antenna plates and the middle plywood layer to reinforce the prototype's structural integrity. Finally, wood-grain contact paper (0.1 mm thick) was applied over the surface, giving the prototype the appearance and texture of a wooden tile. Figure 3 illustrates different stages of the fabrication process. When in use, the side covered with the wood-grain contact paper faces downward toward the underfloor transmitter. The accelerometer and other electronic components were mounted at the center of the panel on the opposite side of the bottom layer and enclosed by an additional thin wood panel.

To facilitate the construction of larger furniture surfaces, we reserved the margins at the edges of the module for screws or nails, allowing attachment to adjacent boards or standard furniture components such as underframes or legs. These margins and screw zones are clearly marked to avoid damaging the antennas. AccelLumber panels can seamlessly integrate with standard wood panels, enabling sensing surfaces of various sizes and shapes. For instance, in circular tabletops, an AccelLumber module can be placed at the center, surrounded by regular wood panels to cover curved areas. Our experiments (Section 6) show that activities on adjacent panels are detected by the AccelLumber panel.

Figure 3: Fabrication process of an AccelLumber panel.(a) RF antennas are affixed to the bottom plywood layer using adhesive and mortise-and-tenon joints, with designated grooves for the PCBs. Note that the spacing between the antennas was determined based on the experimental results presented in the Appendix B. (b) Patch antennas are then placed into cutouts in the top layer, reinforced with polystyrene boards. (c) A wood grain contact paper is applied to the surface to provide the appearance of a wooden tile.

3.3 Underfloor Transmitter

To integrate the transmitter into the floor, we raised the lab floor using several wooden forklift pallets, which were then covered with plywood panels, a material commonly used in flooring applications. The transmitter was placed inside the pallets, approximately 3 cm below the plywood panels (Figure 4). This distance is the minimum required between the transmitter and any covering to ensure proper functionality. The underfloor transmitter (Powercast TX91501B [12]) emits a Direct-Sequence Spread Spectrum (DSSS) RF carrier centered at 915 MHz, with an Effective Isotropic Radiated Power (EIRP) of 3 W. The system complies with Federal Communications Commission (FCC) safety standards, and according to the World Health Organization (WHO), exposure to low-level EM fields does not pose a health risk [64]. Although providing continuous coverage across the entire floor surface would require multiple transmitters, for simplicity, we used a single transmitter our experiments.

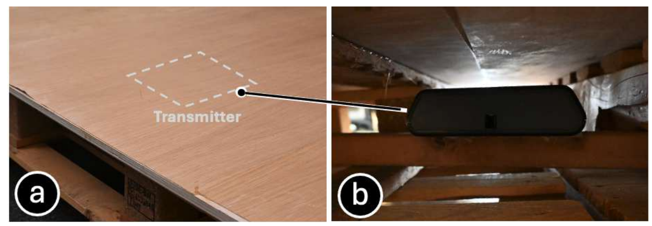

Figure 4: The underfloor transmitter setup: (a) Our lab floor was elevated using wooden forklift pallets covered with plywood panels. (b) The transmitter is positioned within the pallets, approximately 3 cm below the plywood panels.

4 EXPERIMENT 1: PERFORMANCE CHARACTERIZATION

This experiment evaluated the performance of AccelLumber and investigated its ability to reliably power sensors and electronic components. We also explored how AccelLumber can be scaled to different sizes by identifying the minimum number of receiver antennas required for continuous operation and determining the maximum transmitter coverage area, providing insights into power infrastructure needs and overall practicality. Our study primarily focused on desktops and stool seats, and therefore, the experiments were conducted with the antenna array positioned at heights corresponding to the typical dimensions of these furniture items (i.e., up to 50 cm from the floor for stool seats and up to 80 cm from the floor for desktops).

4.1 Apparatus

This experiment involved an antenna array positioned above and facing a raised floor with an embedded transmitter. Four array sizes were tested: 1×2, 1×4, 2×2, and 3×4 (rows $\times$ columns). The corresponding footprints were 36 cm $\times$ 23 cm, 72 cm $\times$ 23 cm, 36 cm $\times$ 46 cm, and 72 cm $\times$ 69 cm (length $\times$ width), with margins equal to half the spacing in each direction.

4.2 Procedure

To evaluate whether AccelLumber can reliably power its embedded electronics, we measured energy harvesting performance with the transmitter placed both within and beyond the footprints of the tested antenna arrays. This setup reflects realistic scenarios where the transmitter is not always perfectly centered. Measurements

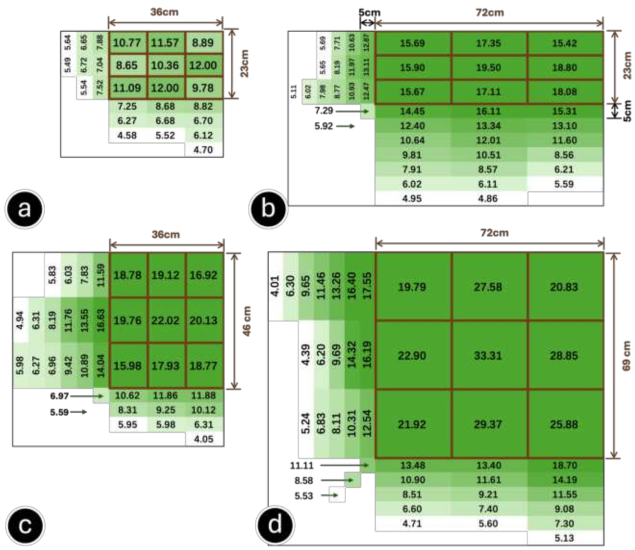

Figure 5: The harvested power recorded with the transmitter positioned 50cm below the tested AccelLumber panels. We measured the energy harvested (in mW) by an underfloor transmitter placed at different locations, both within and beyond the footprint of the tested antenna arrays (the brown grid): (a) 1×2, (b) 1×4, (c) 2×2, and (d) 3×4. The green areas represent locations where the harvested power exceeds the minimum required to operate the AccelLumber system (5.98 mW). The white areas, marked with a number, indicate locations where the harvested power falls just short of 5.98 mW. The footprint of the tested antenna arrays, along with their length and width, is outlined in brown. Outside the footprint boundaries, as marked in (b), each cell corresponds to a 5cm step where power data was collected.

taken with the transmitter positioned outside the array footprints also provided insight into the transmitter's maximum coverage area. Specifically, we divided each array footprint into a 3×3 grid and measured harvested energy with the transmitter centered in each subregion. When measuring with the transmitter near or outside the footprint's boundaries, we first positioned the transmitter along the footprint's edge, with half of the device inside the footprint, and then moved it outward in 5 cm increments, recording harvested energy until it dropped below 5.98 mW, the minimum required to power the sensor and electronics. We repeated this procedure at the panel corners along the diagonal. Additionally, we varied the distance between the transmitter and the antenna array under two conditions: 50cm and 80cm, corresponding to the typical heights of a tabletop and a stool seat, respectively. For each combination of antenna array size and distance, we recorded the voltage and current outputs of the array.

4.3 Results

Our results showed that the harvested energy was approximately symmetric along the four sides of the AccelLumber panel, so we present data from one-quarter of the AccelLumber panel. Figure 5 and Figure 6 show the locations and harvested energy.

4.3.1 *Panel Size Scalability.*

We measured the scalability of AccelLumber panels by determining the minimum number of receiver antennas required for continuous operation. Among the tested configurations, the 1×2 configuration could not harvest sufficient power at the distance of 80cm to meet the system's power requirements of 5.98mW (Figure 6a). However, at 50cm, it successfully harvested enough power, both within and beyond its footprint area (Figure 5a). When the transmitter was placed outside the antenna's footprint area, the antennas provided adequate power up to 15cm in the longitudinal direction and 10cm in the lateral direction. These results suggest that the smallest AccelLumber panels, equipped with 1×2 antennas, can be as small as 36 cm $\times$ 23 cm. Such panels are suitable for integration into furniture surfaces, such as stools, chairs, and coffee tables, which typically have a height of approximately 50 cm.

In contrast, the 1×4 and 2×2 configurations effectively harvested sufficient power at both 50cm and 80cm distances across the array's footprint and beyond (Figure 5b, c and Figure 6b, c). This result suggests that four antennas are necessary to harvest adequate power at a distance of 80cm from the underfloor transmitter. The smallest rectangular panel of AccelLumber, consisting of 2×2 antennas, can be as small as 36 cm $\times$ 46 cm, matching the footprint of the antenna array. A square version can be created by extending the short axis to 46cm, resulting in dimensions of 46cm by 46cm. Aside from shorter furniture like stools and chairs, the AccelLumber panels, consisting of 1×4 and 2×2 arrays, are well-suited for integration into taller surfaces such as tables and desks, which typically have a height of approximately 80cm.

For the 3×4 configuration, the harvested power peaked when the transmitter was centrally positioned on the antenna array for both 50cm and 80cm conditions. At 50cm (the height of stool seats), the average harvested power within the footprint was 25.6mW (SD = 4.3), while at 80cm (the height of tabletops), it was 16.4mW (SD = 0.6), across all nine locations (Figure 5 and 6). Despite some minor variations in harvested power due to the uneven distribution of the RF field, measurements remained relatively stable, particularly at 80cm.

4.3.2 *Transmitter Coverage & Power Infrastructure Requirements.*

Overall, it is promising that all tested antenna array configurations, except the 1×2 configuration at 80 cm height, maintain sufficient power even when the underfloor transmitter is positioned outside the panel's footprint area. For example, in the case of the 3×4 array at the 80 cm condition, as shown in the figure, the array harvested power exceeding the required 5.98 mW when the transmitter was at least 25 cm from the panel edge (center-to-edge distance), with this distance increasing to 30 cm near the central axis of the array. The maximum coverage distance along the diagonal direction was 20 cm, which was shorter compared to other directions. In the 50 cm condition, the maximum safe center-to-edge distance for the transmitter was 20 cm, though this distance could extend to 30 cm near the central axis of the array, following a similar trend as observed in the 80 cm condition. Additionally, we found that the harvested power decreased more significantly along the diagonal direction, with the maximum coverage distance being 10 cm. The increased coverage distance in the 80 cm condition, relative to the 50 cm condition, is attributed to the RF field's reduced coverage

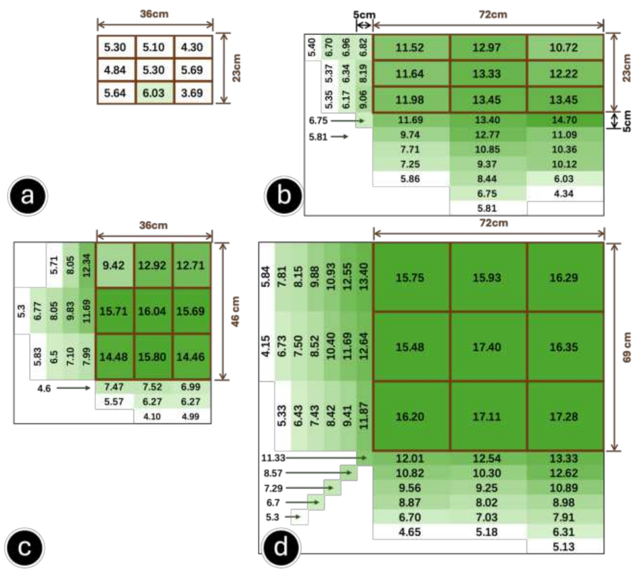

Figure 6: The harvested power recorded with the transmitter positioned 80cm below the tested AccelLumber panels. We measured the energy harvested (in mW) by an underfloor transmitter placed at different locations, both within and beyond the footprint of the tested antenna arrays (the brown grid): (a) 1×2, (b) 1×4, (c) 2×2, and (d) 3×4. The green areas represent locations where the harvested power exceeds the minimum required to operate the AccelLumber system (5.98 mW). The white areas, marked with a number, indicate locations where the harvested power falls just short of 5.98 mW. The footprint of the tested antenna arrays, along with their length and width, is outlined in brown. Outside the footprint boundaries, as marked in (b), each cell corresponds to a 5cm step where power data was collected.

near the transmitter leading to fewer antennas harvesting energy from it.

Considering the power infrastructure, AccelLumber envisions a transmitter grid to provide room-scale coverage for continuous operation (similar to [35, 41]). The study results on the maximum coverage distance beyond the array's footprint provide useful guidance for determining appropriate transmitter spacing within the grid. For instance, in the case of the 3×4 array at the 80 cm condition, the center-to-edge coverage distance is 25 cm. Given the edge of the transmitter is 16 cm, the edge-to-edge distance should be $25 - 16/2 = 17cm$. Therefore, the maximum distance of 17 cm beyond the edge of an AccelLumber panel suggests a rough spacing of one transmitter every 1.2 meters (i.e., $17cm \times 2 + 16cm + 70cm$, center-to-center). In a room measuring $6m \times 6m$, this would translate to a 5×5 transmitter array to ensure continuous power delivery to AccelLumber panels at any location within the room.

It is important to note that energy levels below 5.98 mW do not imply system failure. Instead, they indicate that the harvested power is insufficient to fully sustain the system's continuous consumption needs. In such scenarios, the system can operate temporarily but will eventually require recharging. This approach aligns with use cases involving intermittent rather than continuous activities. The system can be configured to operate during active periods and recharge in preparation for subsequent tasks. While this offers a promising direction for optimizing system design, it lies beyond the scope of this initial exploration, as our system, even without optimization, already achieves adequate power across most tested conditions.

5 DEMO APPLICATIONS

To illustrate the capability of AccelLumber as a building material, we designed and constructed a desk, a drop-leaf table, and a stool using AccelLumber panels with 3×4 receiver antennas. Building these pieces involved woodworking operations such as joining AccelLumber boards edge-to-edge and assembling them with other furniture components, such as desk legs. The completed tables and stool can detect a range of user activities, which we discuss in detail in Section 6.

Desk. We constructed a desk with its surface made from AccelLumber and off-the-shelf desk legs. The desk is 140cm in length, 70cm in depth, and 72cm in height. The desktop was assembled by aligning an AccelLumber board and a standard plywood board edge-to-edge with the aid of 7.7 cm flat brace brackets and #4 screws, a common method for connecting wood panels in modular furniture (Figure 7c). Two brace brackets were positioned 30cm apart along the edge of the boards. Screws were inserted into the empty margins, avoiding areas occupied by antennas. At the corners of the completed desktop panel, we installed the desk legs by first drilling pilot holes and then securing the legs with screws (Figure 7a). The final assembled desk is shown in (Figure 7b). As demonstrated in our experiments in Section 6, activities occurring on the uninstrumented plywood board can also be accurately detected.

Figure 7: Fabrication of a desk using AccelLumber panels. (a) Attach the legs by screwing them into pre-drilled pilot holes within an AccelLumber panel. (b) The completed desk assembly. The dashed box indicates the location of the electronic components (power management, BLE, MCU, and accelerometer) embedded within the panel. (c) The desktop was constructed using two AccelLumber panels joined with flat brace brackets.

Drop leaf table. Using a similar approach, we created a drop leaf table. The AccelLumber panel served as the drop leaf, attached to the tabletop with two self-supporting hinges (Figure 8a). These hinges were secured to the panels with #4 screws. The table leaf (Figure 8b) can be flipped open to create a flat surface (Figure 8c), and this motion is detectable by the AccelLumber's accelerometer. In this example, the main tabletop surface itself was not instrumented using AccelLumber.

Figure 8: Fabrication of a drop-leaf table Using AccelLumber panels. (a) The drop leaf was attached to the tabletop with self-supporting hinges. (b) In the folded position, the drop leaf rests downward. (c) When lifted, the leaf extends to create a larger flat surface. The AccelLumber is capable of detecting the open and close motion of the drop leaf. The dashed box indicates the location of the electronics components embedded within the panel.

Stool. The stool was created with an AccelLumber panel as the seat, supported by four off-the-shelf chair legs, each 40 cm in height (Figure 9a). To increase comfort, an 18 cm thick cushion has been added to the seat (Figure 9c). Note that the placement of the cushion does not impact energy harvesting, as the transmitter is positioned beneath the seat, below the floor.

Figure 9: Fabrication of a stool using an AccelLumber panel. (a) Attach the stool legs by fastening them into the pre-drilled pilot holes in the AccelLumber panel. (b) The finished stool, without a cushion. The dashed box indicates the location of the electronic components embedded within the panel.(c) The stool with a cushion placed on top, which does not obstruct the RF energy emitted from below.

6 EXPERIMENT 2: ACTIVITY RECOGNITION

This experiment aimed to evaluate the activity recognition capabilities of AccelLumber in a furniture context. Previous research has demonstrated the feasibility of using accelerometer data for activity recognition [39]. Building on this, our study focuses on two key objectives unique to AccelLumber: (1) evaluating the recognition accuracy of AccelLumber when embedded within a desk and stool, and (2) assessing recognition accuracy when activities are performed on an adjacent, non-sensing panel connected to the powered AccelLumber panel. The entire study was conducted with the full system, including sensing and data communication, powered wirelessly.

We conducted our study using the desk and stool presented in our demo applications (Section 5). The activities selected for the study were carefully chosen to align with those frequently explored in prior research on activity recognition, which spans diverse contexts such as kitchen [23], office workspaces [29] and workshop [31]. Importantly, these activities remain undetectable by existing battery-free smart wood panels, such as Tagnoo [58].

The desk-related tasks included appliance usage (e.g., water boiler), power tool operations (e.g., drill), cooking activities (e.g., chopping), and work-related activities (e.g., stapling). Continuous operation of the sensor is important for many of these tasks, as it is often necessary to monitor their duration, rather than merely detecting their occurrence [31]. We also incorporated three stool-based actions: sitting, standing, and leg-shaking. Transitions between sitting and standing are particularly relevant for assessing prolonged sitting patterns, which are useful for understanding sedentary behavior and promoting healthier work practices [5]. Additionally, leg-shaking, a common fidgeting behavior, has been shown to be useful in identifying signs of restlessness or stress [17]. While the accelerometer can track AccelLumber's own movements (e.g., opening a drop-leaf table), we excluded these events, as raw data alone suffices for detection without machine learning. The study was conducted with our system powered entirely by harvested RF energy.

6.1 Apparatus

The stool was placed in front of the desk, and the transmitter was positioned between the stool and the desk's left AccelLumber panel to power both the stool and that panel, which captured activity data associated with the desk.

6.2 Objects

We identified several power tools (e.g., sender, jigsaw, drill), appliances (e.g., water boiler, microwave), cooking actions (e.g., chopping, slicing), and work-related events (e.g., writing, erasing, stapling) that are representative of typical events occurring on desk surfaces. Additionally, we included actions performed on stools (e.g., sitting down, standing up, shaking legs while seated).

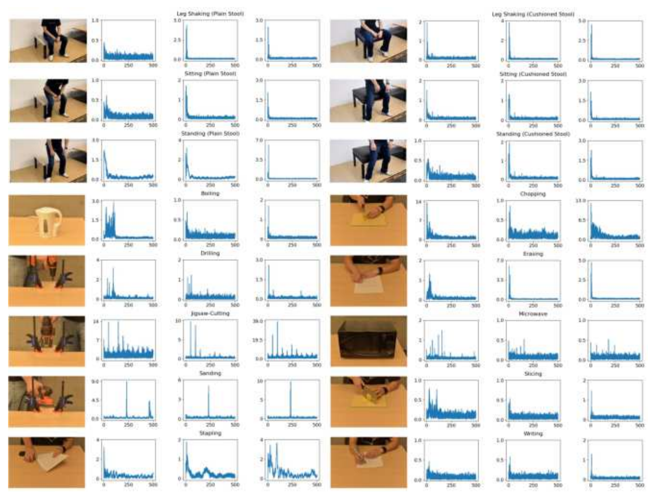

Figure 10: The tested activities and their frequency signatures on the X, Y, and Z directions of the accelerometer. In the signal plots, the X-axis represents frequency and the Y-axis represents magnitude.

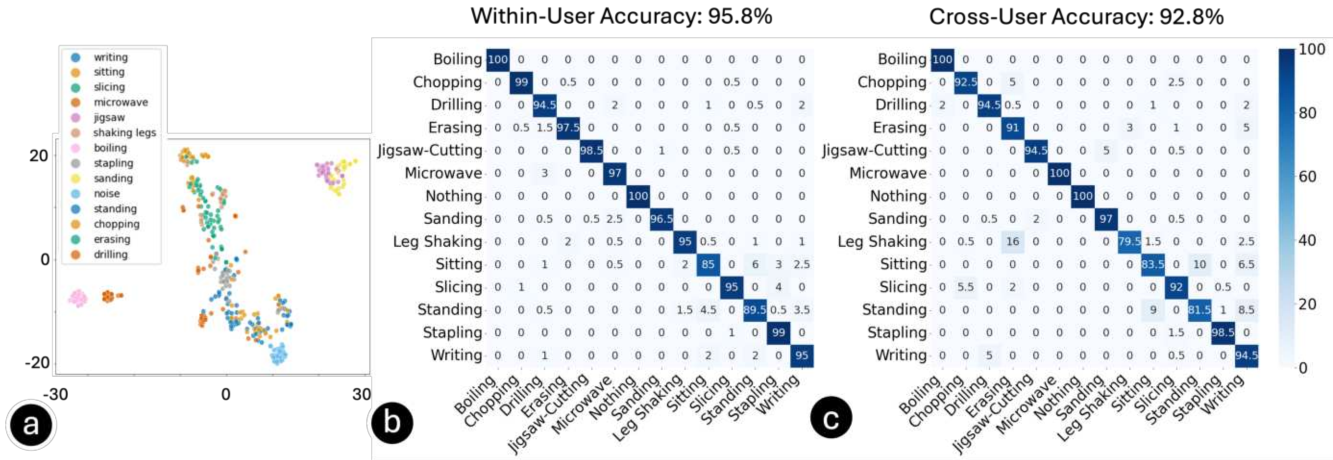

Figure 11: (a) t-SNE plot of the activity data. (b) Confusion matrix showing classification accuracy in the within-user scenario. (c) Confusion matrix showing classification accuracy in the cross-user scenario. All results are based on a model trained using data collected from the desk and stool.

6.3 Data Collection

We recruited 10 participants (5 males and 5 females), aged 24 to 29 years. For each class, we captured 5 seconds of data, with 20 samples collected per participant. In each trial, an activity was randomly selected and performed at random locations and orientations within the testing area. The activities conducted at the desk were carried out 10 times each on both the AccelLumber panel and the adjacent regular wood panel. However, data was recorded only from the accelerometer of the powered panel. The activities performed on the stool were performed 10 times each, both with and without the cushion. For each repetition, participants used a different orientation of the stool. We did not control for environmental factors, such as people walking around tables and stools, to simulate real-world conditions. Figure 10 provides images of each class along with their corresponding frequency signatures. For each class, a total of 200 samples were collected (20 samples $\times$ 10 participants).

6.4 Data Pre-processing and Machine Learning

We employ a preprocessing pipeline to improve the quality of raw accelerometer signals and prepare them for machine learning. First, the DC components of the X, Y, and Z axes are removed to eliminate offsets. Next, a Butterworth low-pass filter with a 450Hz cutoff frequency is applied to preserve activity-relevant frequency components while reducing noise. Using the collected dataset, we trained a machine-learning model with a Random Forest consisting of 1000 decision trees. Based on our observation and initial tests, we derived 33 features per axis across both time and frequency domains. A summary of these features is provided in the appendix.

6.5 Results

The study was successfully completed, with the entire system powered by harvested RF energy. We trained a model using data collected from both the desk and the stool, intentionally diverging from the common approach of training separate models for each item (e.g., one for the desk and one for the stool). This decision was made to push the boundaries of model generalization. This section presents the classification performance of the model, evaluated in terms of both within-user and cross-user accuracy.

6.5.1 Within-User Accuracy. Within-user accuracy represents the prediction accuracy for the model when both the training and testing data were derived from the same user. To evaluate this, we conducted a five-fold cross-validation for each participant, allocating 80% of the data for training and 20% for testing.

The model achieved an accuracy of 95.8% (SD = 4.2%), as shown in Figure 11a. This outcome confirms that most activities associated with the desk and stool produce distinguishable acceleration signals. This is particularly true for activities involving appliances or power tools, which generate distinct signal patterns compared to the user activities performed on the stool. However, the model encountered more difficulties distinguishing stool-related activities, such as Standing and Sitting, which were frequently misclassified as one another and, in some cases, as desk-related activities like Drilling. While we anticipated some confusion between Sitting and Standing due to subtle differences in their signal characteristics, it was unexpected that they were also misclassified as Drilling. We hypothesize that this issue could be mitigated with additional training data. Despite this challenge, several classes, including Boiling, Microwave, Jigsaw-Cutting, Sanding, Drilling, Chopping, Slicing, Stapling, and Writing, achieved an accuracy near or above 95%, which is promising.

The model was trained using data collected from the stool both with and without the cushion, indicating that the cushion’s influence on activity signals is minimal. This is particularly promising, as we initially hypothesized that the cushion, especially the thick one used in our study, might act as a damper and significantly alter the vibration signal patterns, potentially affecting classification accuracy. However, our results demonstrate that the machine-learning model effectively handled these variations in the vibration signals.

Furthermore, our model was trained on data collected from both AccelLumber and regular wood panels and still accurately classified the activities carried out on the regular wood panels. This provides evidence that the AccelLumber panels can be integrated with regular wood panels to form a larger surface while still accurately detecting activities across the entire surface, regardless of whether they occur on or outside the AccelLumber panel.

6.5.2 *Cross-User Accuracy.*

We further evaluated the performance of our model across different users using a leave-one-subject-out cross-validation. In this approach, data from nine participants were used for training, while the data from the remaining participant served as the test set.

The model achieved a cross-user accuracy of 92.8% (SD = 6.8%), as illustrated in Figure 11b. Activities involving appliances and power tools, such as Boiling, Microwave, Jigsaw-Cutting, Sanding, Stapling, and Writing, exhibited accuracies greater than 95%. This can be attributed to the distinct and consistent acceleration patterns generated by the machine, which were more easily distinguishable across different users. As anticipated, user-dependent activities, particularly those involving subtle vibrations such as Sitting, Standing, and Leg Shaking, showed lower accuracy when compared to within-user accuracy. Additionally, there was a higher rate of confusion between desk-related and stool-related activities. Nevertheless, the model maintained relatively high accuracy for most other activities, which is encouraging.

7 LIMITATIONS AND FUTURE WORK

We demonstrated the technical feasibility of a wireless smart wooden panel that integrates conventional sensors and electronic components. In this section, we reflect on the limitations of our approach, discuss the lessons learned from our research, and suggest promising directions for future research.

New Sensors. Our current implementation achieves a 1 kHz sampling and communication rate, supporting the integration of a wide variety of sensors beyond the accelerometer used in this study. Leveraging the MCU, both commodity analog and digital sensors can be incorporated, including light, temperature, humidity, force, gyroscope, and gas sensors. Future work will explore expanding these sensing capabilities, which will allow the detection of a broader range of activities and open new opportunities for smart wooden panels.

Antenna Alignment. Our current implementation requires the transmitter and receiver antennas to be relatively well aligned. A promising direction for future work is to explore techniques that alleviate this requirement. We are investigating alternative powering methods, such as beamforming or omnidirectional transmitter arrays [8, 13], which could potentially allow the system to operate effectively without alignment of the antennas' spatial orientation or polarization characteristics. Future work should also systematically characterize the system's tolerance to practical installation errors, such as lateral offset, angular rotation, and height variation between transmitter and receiver antennas. In addition, it will be important to evaluate how nearby materials and objects, such as metal frames, appliances, or surrounding furniture components, affect RF power transfer performance in real-world environments.

Compatible Furniture. Beyond the desk and stool demonstrated in this work, the floor-mounted transmitter setup supports a broader range of furniture with open-bottom structures that are exposed to open air, such as couches, beds, benches, and TV stands. However, we have not explored furniture items with more complex structures. For instance, multi-tier furniture such as shelving units could have shelf boards below 80 cm that receive sufficient RF exposure within the transmitter grid coverage, as each shelf would be exposed to at least one transmitter. Shelf boards positioned above 80 cm may still harvest RF power, but likely not enough to surpass the 5.98 mW threshold required for continuous operation. Future work will investigate integrating RF transmitters into ceilings or walls to evaluate the effectiveness of this approach for furniture with more complex structures, including those containing drawers. We also plan to examine how specific structural factors, such as multi-level surfaces and larger unsupported spans, influence antenna placement, RF exposure, and sensing reliability. This would help establish a broader design space for wireless smart furniture beyond the relatively simple form factors explored in the current paper.

Installation. Our work provide an initial estimate of the transmitter density required for room-scale operation. Future work will explore a deployment-oriented study that compares several installation strategies, such as underfloor and ceiling-mounted layouts, in terms of material cost, installation time, wiring effort, maintenance accessibility, and required expertise. Such a study could combine quantitative measures with qualitative feedback from woodworkers or installers to clarify the feasibility of our system.

Module Usability. The primary user group for AccelLumber consists of woodworkers, who will utilize AccelLumber panels to create furniture. In our initial investigation, the usability of the AccelLumber, such as its shape, size, and ease of use in assembling various types of furniture, has not yet been validated by woodworkers. Future research will focus on collecting feedback from woodworkers to refine and validate the current design and inform improvements to the usability of AccelLumber panels.

Long-term Stability. Our work demonstrates that the system can continuously power sensing and communication under the tested conditions, but it does not evaluate multi-day or multi-week deployment. In long-term use, several factors may affect stability, including variation in harvested power over time, supercapacitor aging, drift in electronic performance, and gradual changes in the furniture structure or surrounding environment. A useful next step would be a deployment in which instrumented furniture operates continuously over an extended period, while logging harvested power, charge state, sensing uptime, packet loss, and recognition performance. Such a study would clarify whether the current design is sufficiently stable for everyday use and would help reveal failure modes that are difficult to observe in short laboratory evaluations.

Activity Recognition. Our exploration of activity recognition demonstrates the feasibility of AccelLumber, but there is substantial potential for improvement. For example, we assessed recognition performance on two furniture types, desks and stools, but future research could extend this to include other common furniture with large horizontal surfaces, such as coffee tables and beds. Although we trained a general machine learning model for desks and stools, future studies should aim to develop a generalized model that can accommodate a broader range of furniture types with varying structures and form factors. Furthermore, while we evaluated recognition accuracy with a 70 cm × 70 cm panel, future investigations should examine different panel sizes and shapes supported by our system to assess their performance in recognizing both seen and unseen activities. This will provide useful insights into the robustness and generalizability of our system. Finally, we plan to investigate the impact of wood types on accelerometer signals. While we do not anticipate a significant effect on machine learning performance, this remains an important area for further exploration.

Design Opportunities. Finally, while our evaluation focuses on technical feasibility and activity recognition, wireless smart furniture could support a broader range of application scenarios. Beyond recognizing short interaction events, such furniture may enable longer-term behavioral sensing in homes and workplaces, such as detecting stress-related behaviors, or providing context-aware support around everyday activities. Future work will conduct formative design studies, such as workshops or co-design sessions with furniture designers, woodworkers, and end users, to explore how wireless smart wooden panels could be embodied in different furniture forms and everyday settings.

8 CONCLUSION

In this paper, we took a validation-by-implementation [22] approach to demonstrate the technical feasibility of fully wireless, sensor-powered smart wooden panels capable of supporting conventional off-the-shelf sensors and electronic components, including MCUs and BLE modules. We show that these panels can scale from small configurations with just four receiver antennas to larger panels, enabling integration into furniture surfaces of varying sizes. Furthermore, we demonstrate that the power infrastructure supporting these panels is efficient, requiring fewer RF transmitters than might be anticipated. With activity recognition accuracy exceeding 90% across a range of activities, our work highlights the potential to transform everyday furniture into interactive surfaces.

Our work contributes to research on smart materials and environments in multiple ways. First, integrating conventional sensors, electronic components, and wireless energy-harvesting mechanisms into wooden panels opens new opportunities for exploring diverse sensor types and applications. Second, AccelLumber can be realized in different shapes and sizes, enabling larger and more complex interactive environments beyond the table and stool we tested. Finally, embedding the MCU within the panel enables closed-loop interactions by incorporating output mechanisms, fostering more intuitive and engaging smart environments. Overall, we see this research as an important step toward the development of smart furniture and connected living spaces.

References

[1] Ali Abedi, Mohammad Hossein Mazaheri, Omid Abari, and Tim Brecht. 2018. Witag: Rethinking backscatter communication for wifi networks. In *Proceedings of the 17th ACM workshop on hot topics in networks.* 148–154.

[2] Gregory D. Abowd. 2020. The Internet of Materials: A Vision for Computational Materials. *IEEE Pervasive Computing* 19, 2 (2020), 56–62. https://doi.org/10.1109/MPRV.2020.2982475

[3] Nivedita Arora, Steven L. Zhang, Fereshteh Shahmiri, Diego Osorio, Yi-Cheng Wang, Mohit Gupta, Zhengjun Wang, Thad Starner, Zhong Lin Wang, and Gregory D. Abowd. 2018. SATURN: A Thin and Flexible Self-Powered Microphone Leveraging Triboelectric Nanogenerator. *Proc. ACM Interact. Mob. Wearable Ubiquitous Technol.* 2, 2, Article 60 (jul 2018), 28 pages. https://doi.org/10.1145/3214263

[4] Surajit Das Barman, Ahmed Wasif Reza, Narendra Kumar, Md Ershadul Karim, and Abu Bakar Munir. 2015. Wireless powering by magnetic resonant coupling: Recent trends in wireless power transfer system and its applications. *Renewable and Sustainable energy reviews* 51 (2015), 1525–1552.

[5] Aviroop Biswas, Paul I Oh, Guy E Faulkner, Ravi R Bajaj, Michael A Silver, Marc S Mitchell, and David A Alter. 2015. Sedentary time and its association with risk for disease incidence, mortality, and hospitalization in adults: a systematic review and meta-analysis. *Annals of internal medicine* 162, 2 (2015), 123–132.

[6] Muhammad Umaid Bukhari, Kashif Riaz, Tauseef Tauqeer, and Memoon Sajid. 2019. Simple and low cost triboelectric nanogenerator (TENG) for resource limited environment. In *2019 International Conference on Robotics and Automation in Industry (ICRAI).* 1–4. https://doi.org/10.1109/ICRAI47710.2019.8967354

[7] Mike Burmester and Breno De Medeiros. 2008. The security of EPC Gen2 compliant RFID protocols. In *Applied Cryptography and Network Security: 6th International Conference, ACNS 2008, New York, NY, USA, June 3-6, 2008. Proceedings 6.* Springer, 490–506.

[8] Dingzhao Chen, Yanhui Liu, Ming Li, Pan Guo, Zhuo Zeng, Jun Hu, and Y Jay Guo. 2022. A polarization programmable antenna array. *Engineering* 16 (2022), 100–114.

[9] Tinghai Cheng, Jiajia Shao, and Zhong Lin Wang. 2023. Triboelectric nanogenerators. *Nature Reviews Methods Primers* 3, 1 (2023), 39.

[10] Gabe Cohn, Daniel Morris, Shwetak N. Patel, and Desney S. Tan. 2011. Your Noise is My Command: Sensing Gestures Using the Body as an Antenna. In *Proceedings of the SIGCHI Conference on Human Factors in Computing Systems* (Vancouver, BC, Canada) *(CHI '11).* Association for Computing Machinery, New York, NY, USA, 791–800. https://doi.org/10.1145/1978942.1979058

[11] Diane Cook and Sajal Das. 2004. *Smart Environments: Technology, Protocols and Applications (Wiley Series on Parallel and Distributed Computing).* Wiley-Interscience, USA.

[12] Powercast Corporation. 2021. *User Manual: TX91501B Powercaster Transmitter (Revision A).* https://www.powercastco.com/wp-content/uploads/2021/06/User-Manual-TX-915-01B-Rev-A-1.pdf Accessed: 2024-12-01.

[13] Xiaoran Fan, Han Ding, Sugang Li, Michael Sanzari, Yanyong Zhang, Wade Trappe, Zhu Han, and Richard E Howard. 2018. Energy-ball: Wireless power transfer for batteryless internet of things through distributed beamforming. *Proceedings of the ACM on Interactive, Mobile, Wearable and Ubiquitous Technologies* 2, 2 (2018), 1–22.

[14] Jun Gong, Yu Wu, Lei Yan, Teddy Seyed, and Xing-Dong Yang. 2019. Tessutivo: Contextual interactions on interactive fabrics with inductive sensing. In *Proceedings of the 32nd Annual ACM Symposium on User Interface Software and Technology.* 29–41.

[15] Agrim Gupta, Daegue Park, Shayaun Bashar, Cédric Girerd, Nagarjun Bhat, Siddhi Mundhra, Tania K Morimoto, and Dinesh Bharadia. 2023. ForceSticker: Wireless, Batteryless, Thin & Flexible Force Sensors. *Proceedings of the ACM on Interactive, Mobile, Wearable and Ubiquitous Technologies* 7, 1 (2023), 1–32.

[16] Sidhant Gupta, Matthew S. Reynolds, and Shwetak N. Patel. 2010. ElectriSense: Single-point Sensing Using EMI for Electrical Event Detection and Classification in the Home. In *Proceedings of the 12th ACM International Conference on Ubiquitous Computing* (Copenhagen, Denmark) *(UbiComp '10).* ACM, New York, NY, USA, 139–148. https://doi.org/10.1145/1864349.1864375

[17] Unsoo Ha, Sohrab Madani, and Fadel Adib. 2021. WiStress: Contactless stress monitoring using wireless signals. *Proceedings of the ACM on Interactive, Mobile, Wearable and Ubiquitous Technologies* 5, 3 (2021), 1–37.

[18] Saifei Hao, Jingyi Jiao, Yandong Chen, Zhong Lin Wang, and Xia Cao. 2020. Natural wood-based triboelectric nanogenerator as self-powered sensing for smart homes and floors. *Nano Energy* 75 (2020), 104957.

[19] Chris Harrison and Scott E Hudson. 2008. Scratch input: creating large, inexpensive, unpowered and mobile finger input surfaces. In *Proceedings of the 21st annual ACM symposium on User interface software and technology.* 205–208.

[20] D Hoffmann, A Willmann, R Göpfert, P Becker, B Folkmer, and Y Manoli. 2013. Energy harvesting from fluid flow in water pipelines for smart metering applications. In *Journal of Physics: Conference Series*, Vol. 476. IOP Publishing, 012104.

[21] Meng-Ju Hsieh, Jr-Ling Guo, Chin-Yuan Lu, Han-Wei Hsieh, Rong-Hao Liang, and Bing-Yu Chen. 2019. RFTouchPads: Batteryless and wireless modular touch sensor pads based on RFID. In *Proceedings of the 32nd Annual ACM Symposium on User Interface Software and Technology.* 999–1011.

[22] Scott E Hudson and Jennifer Mankoff. 2014. Concepts, values, and methods for technical human–computer interaction research. In *Ways of Knowing in HCI.* Springer, 69–93.

[23] Yasha Iravantchi, Yi Zhao, Kenrick Kin, and Alanson P. Sample. 2023. SAWSense: Using Surface Acoustic Waves for Surface-Bound Event Recognition. In *Proceedings of the 2023 CHI Conference on Human Factors in Computing Systems* (Hamburg, Germany) *(CHI '23).* Association for Computing Machinery, New York, NY, USA, Article 422, 18 pages. https://doi.org/10.1145/3544548.3580991

[24] Ayaka Ishii, Kunihiro Kato, Kaori Ikematsu, Yoshihiro Kawahara, and Itiro Siio. 2022. Circwood: laser printed circuit boards and sensors for affordable DIY woodworking. In *Proceedings of the Sixteenth International Conference on Tangible, Embedded, and Embodied Interaction.* 1–11.

[25] Kiyoshi Itao. 2007. Wearable Sensor Network Connecting Artifacts, Nature and Human Being. In *SENSORS, 2007 IEEE.* 1120–1123. https://doi.org/10.1109/ICSENS.2007.4388603

[26] Lasse Kaila, Henrik Raula, Miika Valtonen, and Karri Palovuori. 2012. Living wood: a self-hiding calm user interface. In *Proceeding of the 16th International Academic MindTrek Conference*. 267–274.

[27] Saman Kuntharin, Viyada Harnchana, Jirapan Sintusiri, Prasit Thongbai, Annop Klamchuen, Kitiphat Sinthiptharakoon, Vittaya Amornkitbamrung, and Prinya Chindaprasirt. 2023. Smart triboelectric floor based on calcium silicate-carbon composite for energy harvesting and motion sensing applications. *Sensors and Actuators A: Physical* 358 (2023), 114423.

[28] Zhihui Lai, Junchen Xu, Chris R Bowen, and Shengxi Zhou. 2022. Self-powered and self-sensing devices based on human motion. *Joule* 6, 7 (2022), 1501–1565.

[29] Gierad Laput and Chris Harrison. 2019. Sensing fine-grained hand activity with smartwatches. In *Proceedings of the 2019 CHI Conference on Human Factors in Computing Systems*. 1–13.

[30] Gierad Laput and Chris Harrison. 2019. SurfaceSight: A New Spin on Touch, User, and Object Sensing for IoT Experiences. In *Proceedings of the 2019 CHI Conference on Human Factors in Computing Systems* (Glasgow, Scotland Uk) *(CHI '19)*. Association for Computing Machinery, New York, NY, USA, 1–12. https://doi.org/10.1145/3290605.3300559

[31] Gierad Laput, Robert Xiao, and Chris Harrison. 2016. Viband: High-fidelity bio-acoustic sensing using commodity smartwatch accelerometers. In *Proceedings of the 29th Annual Symposium on User Interface Software and Technology*. 321–333.

[32] Gierad Laput, Yang Zhang, and Chris Harrison. 2017. Synthetic Sensors: Towards General-Purpose Sensing. In *Proceedings of the 2017 CHI Conference on Human Factors in Computing Systems* (Denver, Colorado, USA) *(CHI '17)*. Association for Computing Machinery, New York, NY, USA, 3986–3999. https://doi.org/10.1145/3025453.3025773

[33] Jianchao Li, Fanghui Yin, Liming Wang, Bin Cui, and Daiming Yang. 2019. Electromagnetic induction position sensor applied to anti-misalignment wireless charging for UAVs. *IEEE Sensors Journal* 20, 1 (2019), 515–524.

[34] Tianxing Li, Qiang Liu, and Xia Zhou. 2016. Practical Human Sensing in the Light. In *Proceedings of the 14th Annual International Conference on Mobile Systems, Applications, and Services* (Singapore, Singapore) *(MobiSys '16)*. Association for Computing Machinery, New York, NY, USA, 71–84. https://doi.org/10.1145/2906388.2906401

[35] Ying Li and Vikram Jandhyala. 2011. Design of retrodirective antenna arrays for short-range wireless power transmission. *IEEE Transactions on Antennas and Propagation* 60, 1 (2011), 206–211.

[36] Yichen Li, Tianxing Li, Ruchir A Patel, Xing-Dong Yang, and Xia Zhou. 2018. Self-powered gesture recognition with ambient light. In *Proceedings of the 31st annual ACM symposium on user interface software and technology*. 595–608.

[37] Zihe Li, James Roscow, Hamideh Khanbareh, Geoff Haswell, and Chris Bowen. 2024. Energy harvesting from water flow by using piezoelectric materials. *Advanced Energy and Sustainability Research* 5, 5 (2024), 2300235.

[38] Wenzhou Lin, Yuchen Wei, Xupeng Wang, Kangjia Zhai, and Xiaomin Ji. 2023. Study on human motion energy harvesting devices: A review. *Machines* 11, 10 (2023), 977.

[39] Jian Liu, Yingying Chen, Marco Gruteser, and Yan Wang. 2017. Vibsense: Sensing touches on ubiquitous surfaces through vibration. In *2017 14th Annual IEEE International Conference on Sensing, Communication, and Networking (SECON)*. IEEE, 1–9.

[40] Jianjun Luo, Ziming Wang, Liang Xu, Aurelia Chi Wang, Kai Han, Tao Jiang, Qingsong Lai, Yu Bai, Wei Tang, Feng Ru Fan, et al. 2019. Flexible and durable wood-based triboelectric nanogenerators for self-powered sensing in athletic big data analytics. *Nature communications* 10, 1 (2019), 5147.

[41] Andrea Massa, Giacomo Oliveri, Federico Viani, and Paolo Rocca. 2013. Array designs for long-distance wireless power transmission: State-of-the-art and innovative solutions. *Proc. IEEE* 101, 6 (2013), 1464–1481.

[42] Yogesh Kumar Meena, Krishna Seunarine, Deepak Ranjan Sahoo, Simon Robinson, Jennifer Pearson, Chi Zhang, Matt Carnie, Adam Pockett, Andrew Prescott, Suzanne K Thomas, et al. 2020. PV-tiles: towards closely-coupled photovoltaic and digital materials for useful, beautiful and sustainable interactive surfaces. In *Proceedings of the 2020 CHI Conference on Human Factors in Computing Systems*. 1–12.

[43] Inc. mui Lab. 2017. *The smart home Mui Board*. Retrieved April 2, 2024 from https://muilab.com/

[44] C.D. Nugent, S.I. McClean, I. Cleland, and W. Burns. 2014. 13.18 - Sensor Technology for a Safe and Smart Living Environment for the Aged and Infirm at Home. In *Comprehensive Materials Processing*, Saleem Hashmi, Gilmar Ferreira Batalha, Chester J. Van Tyne, and Bekir Yilbas (Eds.). Elsevier, Oxford, 459–472. https://doi.org/10.1016/B978-0-08-096532-1.01319-4

[45] Simon Olberding, Nan-Wei Gong, John Tiab, Joseph A Paradiso, and Jürgen Steimle. 2013. A cuttable multi-touch sensor. In *Proceedings of the 26th annual ACM symposium on User interface software and technology*. 245–254.

[46] Shijia Pan, Ceferino Gabriel Ramirez, Mostafa Mirshekari, Jonathon Fagert, Albert Jin Chung, Chih Chi Hu, John Paul Shen, Hae Young Noh, and Pei Zhang. 2017. Surfacevibe: vibration-based tap & swipe tracking on ubiquitous surfaces. In *Proceedings of the 16th ACM/IEEE International Conference on Information Processing in Sensor Networks*. 197–208.

[47] Patrick Parzer, Florian Perteneder, Kathrin Probst, Christian Rendl, Joanne Leong, Sarah Schuetz, Anita Vogl, Reinhard Schwoediauer, Martin Kaltenbrunner, Siegfried Bauer, et al. 2018. Resi: A highly flexible, pressure-sensitive, imperceptible textile interface based on resistive yarns. In *Proceedings of the 31st Annual ACM Symposium on User Interface Software and Technology*. 745–756.

[48] Minu A Pillai and Ezhilarasi Deenadayalan. 2014. A review of acoustic energy harvesting. *International journal of precision engineering and manufacturing* 15 (2014), 949–965.

[49] Ivan Poupyrev, Nan-Wei Gong, Shiho Fukuhara, Mustafa Emre Karagozler, Carsten Schwesig, and Karen E. Robinson. 2016. Project Jacquard: Interactive Digital Textiles at Scale. In *Proceedings of the 2016 CHI Conference on Human Factors in Computing Systems (CHI '16)*. Association for Computing Machinery, New York, NY, USA, 4216–4227. https://doi.org/10.1145/2858036.2858176

[50] Powercast Corporation. 2024. Powercast Corporation: Wireless Power Solutions. https://www.powercastco.com/. Accessed: 2024-12-10.

[51] Shuibao Qi, Mourad Oudich, Yong Li, and Badreddine Assouar. 2016. Acoustic energy harvesting based on a planar acoustic metamaterial. *Applied Physics Letters* 108, 26 (2016).

[52] Vaishnavi Ranganathan, Sidhant Gupta, Jonathan Lester, Joshua R Smith, and Desney Tan. 2018. Rf bandaid: A fully-analog and passive wireless interface for wearable sensors. *Proceedings of the ACM on Interactive, Mobile, Wearable and Ubiquitous Technologies* 2, 2 (2018), 1–21.

[53] Takuya Sasatani, Alanson P Sample, and Yoshihiro Kawahara. 2021. Room-scale magnetoquasistatic wireless power transfer using a cavity-based multimode resonator. *Nature Electronics* 4, 9 (2021), 689–697.

[54] Yu Shao, Xinyue Wang, Wenjie Song, Sobia Ilyas, Haibo Guo, and Wen-Shao Chang. 2021. Feasibility of using floor vibration to detect human falls. *International journal of environmental research and public health* 18, 1 (2021), 200.

[55] Zhihui Shao, Mohammad A. Islam, and Shaolei Ren. 2020. Your Noise, My Signal: Exploiting Switching Noise for Stealthy Data Exfiltration from Desktop Computers. *Proc. ACM Meas. Anal. Comput. Syst.* 4, 1, Article 07 (may 2020), 39 pages. https://doi.org/10.1145/3379473

[56] Yonghao Shi, Chenzheng Li, Yuning Su, Xing-Dong Yang, and Te-Yen Wu. 2024. WooDowel: Electrode Isolation for Electromagnetic Shielding in Triboelectric Plywood Sensors. In *Proceedings of the CHI Conference on Human Factors in Computing Systems*. 1–17.

[57] Yuning Su, Yonghao Shi, Da-Yuan Huang, and Xing-Dong Yang. 2023. Laser-PoweredVibrotactileRendering. In *Adjunct Proceedings of the 36th Annual ACM Symposium on User Interface Software and Technology*. 1–3.

[58] Yuning Su, Tingyu Zhang, Jiuen Feng, Yonghao Shi, Xing-Dong Yang, and Te-Yen Wu. 2024. Tagnoo: Enabling Smart Room-Scale Environments with RFID-Augmented Plywood. In *Proceedings of the CHI Conference on Human Factors in Computing Systems*. 1–18.

[59] Saiganesh Swaminathan, Jonathon Fagert, Michael Rivera, Andrew Cao, Gierad Laput, Hae Young Noh, and Scott E Hudson. 2020. Optistructures: Fabrication of room-scale interactive structures with embedded fiber bragg grating optical sensors and displays. *Proceedings of the ACM on Interactive, Mobile, Wearable and Ubiquitous Technologies* 4, 2 (2020), 1–21.

[60] Yen Kheng Tan and Sanjib Kumar Panda. 2010. Energy harvesting from hybrid indoor ambient light and thermal energy sources for enhanced performance of wireless sensor nodes. *IEEE Transactions on Industrial Electronics* 58, 9 (2010), 4424–4435.

[61] Shan-Yuan Teng, KD Wu, Jacqueline Chen, and Pedro Lopes. 2022. Prolonging VR haptic experiences by harvesting kinetic energy from the user. In *Proceedings of the 35th Annual ACM Symposium on User Interface Software and Technology*. 1–18.

[62] Nguyen Van Huynh, Nguyen Quang Hieu, Nam H Chu, Diep N Nguyen, Dinh Thai Hoang, and Eryk Dutkiewicz. 2023. Defeating eavesdroppers with ambient backscatter communications. In *2023 IEEE Wireless Communications and Networking Conference (WCNC)*. IEEE, 1–6.

[63] Raphael Wimmer, Matthias Kranz, Sebastian Boring, and Albrecht Schmidt. 2007. Captable and capshelf-unobtrusive activity recognition using networked capacitive sensors. In *2007 Fourth International Conference on Networked Sensing Systems*. IEEE, 85–88.

[64] World Health Organization (WHO). 2016. Radiation: Electromagnetic Fields - Questions and Answers. https://www.who.int/news-room/questions-and-answers/item/radiation-electromagnetic-fields Accessed: 2024-12-01.

[65] Changsheng Wu, Aurelia C Wang, Wenbo Ding, Hengyu Guo, and Zhong Lin Wang. 2019. Triboelectric nanogenerator: a foundation of the energy for the new era. *Advanced Energy Materials* 9, 1 (2019), 1802906.

[66] Te-Yen Wu, Shutong Qi, Junchi Chen, MuJie Shang, Jun Gong, Teddy Seyed, and Xing-Dong Yang. 2020. Fabriccio: Touchless Gestural Input on Interactive Fabrics. In *Proceedings of the 2020 CHI Conference on Human Factors in Computing Systems* (Honolulu, HI, USA) *(CHI '20)*. Association for Computing Machinery, New York, NY, USA, 1–14. https://doi.org/10.1145/3313831.3376681

[67] Te-Yen Wu, Lu Tan, Yuji Zhang, Teddy Seyed, and Xing-Dong Yang. 2020. Capacitivo: Contact-Based Object Recognition on Interactive Fabrics using Capacitive Sensing. In *Proceedings of the 33nd Annual ACM Symposium on User Interface*

Software and Technology (UIST '20). Association for Computing Machinery, New York, NY, USA. https://doi.org/doi.org/10.1145/3379337.3415829 event-place: Virtual Event.
[68] Te-Yen Wu and Xing-Dong Yang. 2022. iWood: Makeable Vibration Sensor for Interactive Plywood. In Proceedings of the 35th Annual ACM Symposium on User Interface Software and Technology. 1–12.
[69] Robert Xiao, Greg Lew, James Marsanico, Divya Hariharan, Scott Hudson, and Chris Harrison. 2014. Toffee: enabling ad hoc, around-device interaction with acoustic time-of-arrival correlation. In Proceedings of the 16th international conference on Human-computer interaction with mobile devices & services. 67–76.
[70] Yuanming Zeng, Huijing Xiang, Ning Zheng, Xia Cao, Ning Wang, and Zhong Lin Wang. 2022. Flexible triboelectric nanogenerator for human motion tracking and gesture recognition. Nano Energy 91 (2022), 106601.
[71] Dingtian Zhang, Canek Fuentes-Hernandez, Raaghesh Vijayan, Yang Zhang, Yunzhi Li, Jung Wook Park, Yiyang Wang, Yuhui Zhao, Nivedita Arora, Ali Mirzazadeh, Youngwook Do, Tingyu Cheng, Saiganesh Swaminathan, Thad Starner, Trisha L. Andrew, and Gregory D. Abowd. 2022. Flexible computational photodetectors for self-powered activity sensing. npj Flexible Electronics 6, 1 (Jan. 2022), 7. https://doi.org/10.1038/s41528-022-00137-z
[72] Dingtian Zhang, Jung Wook Park, Yang Zhang, Yuhui Zhao, Yiyang Wang, Yunzhi Li, Tanvi Bhagwat, Wen-Fang Chou, Xiaojia Jia, Bernard Kippelen, et al. 2020. OptoSense: Towards ubiquitous self-powered ambient light sensing surfaces. Proceedings of the ACM on interactive, mobile, wearable and ubiquitous technologies 4, 3 (2020), 1–27.
[73] Pengyu Zhang, Dinesh Bharadia, Kiran Joshi, and Sachin Katti. 2016. Hitchhike: Practical backscatter using commodity wifi. In Proceedings of the 14th ACM conference on embedded network sensor systems CD-ROM. 259–271.
[74] Yang Zhang, Yasha Iravantchi, Haojian Jin, Swarun Kumar, and Chris Harrison. 2019. Sozu: Self-Powered Radio Tags for Building-Scale Activity Sensing. In Proceedings of the 32nd Annual ACM Symposium on User Interface Software and Technology (New Orleans, LA, USA) (UIST '19). Association for Computing Machinery, New York, NY, USA, 973–985. https://doi.org/10.1145/3332165.3347952
[75] Yang Zhang, Gierad Laput, and Chris Harrison. 2018. Vibrosight: Long-Range Vibrometry for Smart Environment Sensing. In Proceedings of the 31st Annual ACM Symposium on User Interface Software and Technology (Berlin, Germany) (UIST '18). Association for Computing Machinery, New York, NY, USA, 225–236. https://doi.org/10.1145/3242587.3242608
[76] Yang Zhang, Chouchang (Jack) Yang, Scott E. Hudson, Chris Harrison, and Alanson Sample. 2018. Wall++: Room-Scale Interactive and Context-Aware Sensing. In Proceedings of the 2018 CHI Conference on Human Factors in Computing Systems (Montreal QC, Canada) (CHI '18). Association for Computing Machinery, New York, NY, USA, 1–15. https://doi.org/10.1145/3173574.3173847

A Appendix: Machine Learning Features

Domain	Features
Frequency	abs energy, absolute maximum, last location of maximum, first location of maximum, maximum, mean, mean abs change, mean change, mean second derivative central, median, minimum, absolute sum of changes, mean n absolute max(3), variance larger than standard deviation, count above mean
Time	rms, zero crossing rate, slope changes, skewness, kurtosis, signal duration, count positive pulses, count negative pulses, average positive pulse intensity, average negative pulse intensity

Table 1: Features used to train our machine learning models.

B Appendix: Antenna Spacing Experiments

Our experiments aimed to investigate how the spacing of receiver antennas affects energy harvesting efficiency, with the goal of informing and improving our implementation. In theory, adjacent antennas should be spaced at least half a wavelength apart ($\lambda/2$) to reduce mutual interference. At our operating frequency of 915 MHz, this distance is approximately 16.4 cm. However, the receiver antenna is 18 cm along its long edge, making $\lambda/2$ spacing infeasible. Simply placing the antennas side by side would likely exacerbate interference (as shown in our experiments). To address this, we systematically explored a range of antenna spacings and their influence on energy harvesting performance.

Given the vast number of potential antenna configurations, exhaustive testing was not feasible. To simplify the approach, we adopted a method similar to prior work [58], employing a test setup with a simplified array of three antennas arranged in either a column or a row. This configuration allowed us to assess the interference between adjacent antennas by measuring the power harvested by the central antenna.

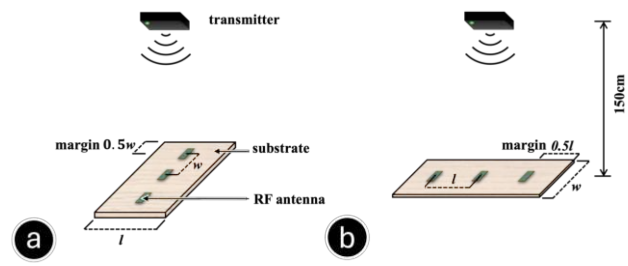

Figure 12: The experiment setup for (a) a 3×1 antenna array and (b) a 1×3 antenna array.

We evaluated energy harvesting efficiency while also accounting for the antenna array's footprint, which directly influences the overall panel size. Specifically, we assessed efficiency in terms of the array's power density (mW/m^2), which is defined as the total power harvested by the array divided by the surface area of the wood panel that it occupies. This metric measures how effectively the array utilizes its allocated area. A higher power density indicates more efficient use of the antenna array relative to its physical coverage, even though it may not necessarily correspond to the absolute maximum harvested power. In our calculations, the footprint includes margins of half the spacing in both the longitudinal and lateral directions (Figure 12). Incorporating these margins ensures that the power density results can be generalized to larger antenna arrays extended along either direction.

B.1 Experiment 3: Effect of Spacing Along the Longitudinal Axis

This experiment examined how varying the spacing distance between adjacent antennas along the longitudinal axis affects both the adjacent antenna interference and power density.

B.1.1 Apparatus.

The study involved using a simplified version of prototype with only three antennas (Powercast 915 MHz, $18cm \times 5cm$) arranged in a 3×1 (row × column) (Figure 12a) configuration, with both the receiver and transmitter antennas aligned in parallel. The antenna array was placed on a desk, with the transmitter mounted approximately 1.5 meters above the array's center. For simplicity, we did not position the transmitter beneath the floor, as our primary goal was to investigate trends in interference and power density variations. These trends are not expected to be strongly influenced by changes in the transmitter's placement. Similarly, while other distances between the transmitter and the array could also be suitable, we expect the overall trends to remain consistent regardless of the specific distance chosen. We used a multimeter (Fluke F17B+) and power profiler (Nordic Power Profiler Kit II) to measure the voltage and current of the antenna array.

B.1.2 Procedure.
We varied the center-to-center distance between adjacent antennas from 19cm to 38cm in 1cm increments. For each tested distance, we measured the total energy harvested by all three antennas and calculated the corresponding power density. Additionally, we measured the energy harvested by the central antenna, which was primarily influenced by interference from the other two antennas.

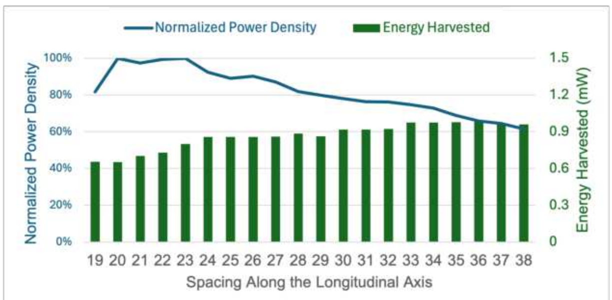

Figure 13: The effect of longitudinal spacing on the energy harvested by the central antenna (green bars, y-axis on the right), and power density (blue line, y-axis on the left) for the 3-antenna array.

B.1.3 Results.
Figure 13 illustrates the energy harvested by the central antenna and the normalized power density. The results indicate that interference persists even when the spacing distance exceeds half the wavelength (16.8 cm). However, the interference diminishes when the spacing exceeds a relatively long distance of 33 cm, though this is also the point where the power density approaches its minimum. In contrast, the power density peaks at spacing distances between 20 cm and 23 cm, followed by a steady decline beyond 23 cm. The results illustrate the trade-off involved in prioritizing power density, which is relatively minor, as the interference at the peak power density is slightly higher than the minimal interference observed at distances of 33 cm or greater. At a 33 cm spacing, the harvested power is reduced by only 9.1% compared to a 23 cm spacing. Although the power density is similar at 20 cm and 23 cm spacings, the reduced interference at 23 cm may enable greater energy harvesting. Therefore, we selected a longitudinal spacing of 23 cm for our final implementation and all experiments.

B.2 Experiment 4: Effect of Spacing Along the Lateral Axis

The goal of this experiment was to evaluate how the spacing between adjacent antennas along the lateral axis influences interference and power density.

B.2.1 Apparatus. The study apparatus was similar to that used in Experiment 1, with the difference being the configuration of the antenna arrays, which were arranged in a 1×3 (row $\times$ column) format (Figure 12b).

B.2.2 Procedure. We varied the center-to-center distance between the antennas from 17cm to 25cm in 1cm increments. This range was chosen to exclude distances smaller than half the wavelength (16.8 cm), as such distances are known to introduce strong interference.

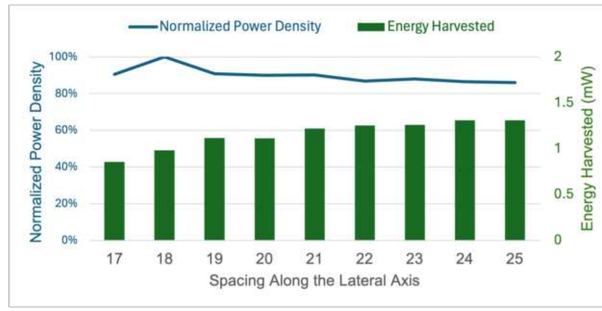

Figure 14: The effect of lateral spacing on the energy harvested by the central antenna (green bars, y-axis on the right) and power density (blue line, y-axis on the left) for the 3-antenna array.

B.2.3 Results. Figure 14 illustrates the energy harvested by the central antenna and the normalized power density. The power density reaches its peak at 18 cm, decreases, and begins to stabilize beyond 22cm. The interference to the central antenna continues to decrease beyond half the wavelength, extending up to 24cm, as the power harvested by the central antenna increases. The tradeoff of prioritizing power density by selecting an 18 cm spacing results in a 24.3% reduction in harvested energy compared to the 24 cm spacing, which yields the maximum power among the tested distances. However, the 18 cm spacing offers the advantage of a smaller footprint, allowing for more compact designs of AccelLumber panels. Additionally, it facilitates the integration of more antennas within a fixed panel size, which can increase the total harvested power. Therefore, we selected a lateral spacing of 18 cm for our final implementation and all experiments.